AD_____

Award Number: W81XWH-09-1-0300

TITLE: The Mechanism of Action of Unique Small Molecules That Inhibit the Pim Protein Kinase Blocking Prostate Cancer Cell Growth

PRINCIPAL INVESTIGATOR: Dr. Andrew Kraft

CONTRACTING ORGANIZATION: Medical University of South Carolina
Charleston, SC 29425

REPORT DATE: May 2011

TYPE OF REPORT: Annual

PREPARED FOR: U.S. Army Medical Research and Materiel Command
Fort Detrick, Maryland 21702-5012

REPORT DOCUMENTATION PAGE

Form Approved
OMB No. 0704-0188

1. REPORT DATE *(DD-MM-YYYY)*	**2. REPORT TYPE**	**3. DATES COVERED** *(From - To)*
01-05-2011	Annual	1 MAY 2010 - 30 APR 2011

4. TITLE AND SUBTITLE

The Mechanism of Action of Unique Small Molecules That Inhibit the Pim Protein Kinase Blocking Prostate Cancer Cell Growth

5a. CONTRACT NUMBER

5b. GRANT NUMBER
W81XWH-09-1-0300

5c. PROGRAM ELEMENT NUMBER

6. AUTHOR(S)
Dr. Andrew Kraft

E-Mail: kraft@musc.edu

5d. PROJECT NUMBER

5e. TASK NUMBER

5f. WORK UNIT NUMBER

7. PERFORMING ORGANIZATION NAME(S) AND ADDRESS(ES)
Medical University of South Carolina
Charleston, SC 29425

8. PERFORMING ORGANIZATION REPORT NUMBER

9. SPONSORING / MONITORING AGENCY NAME(S) AND ADDRESS(ES)
U.S. Army Medical Research and Materiel Command
Fort Detrick, Maryland 21702-5012

10. SPONSOR/MONITOR'S ACRONYM(S)

11. SPONSOR/MONITOR'S REPORT NUMBER(S)

12. DISTRIBUTION / AVAILABILITY STATEMENT
Approved for Public Release; Distribution Unlimited

13. SUPPLEMENTARY NOTES

14. ABSTRACT

Abstract on next page.

15. SUBJECT TERMS

Pim kinases, prostate cancer, cell cycle, kinase inhibitors, SKP-2, p27

16. SECURITY CLASSIFICATION OF:			**17. LIMITATION OF ABSTRACT**	**18. NUMBER OF PAGES**	**19a. NAME OF RESPONSIBLE PERSON**
a. REPORT	**b. ABSTRACT**	**c. THIS PAGE**			USAMRMC
U	U	U	UU	26	**19b. TELEPHONE NUMBER** *(include area code)*

14. ABSTRACT

The Pim protein kinase is over expressed in prostate cancers. To clarify the role of this protein in regulating prostate cancer growth we have investigated its mechanism of action. Additionally, we have studied the ability of small molecule inhibitors of Pim developed in our laboratory to block the growth stimulatory affects of this protein kinase. We find that Pim-1 is able to decrease the levels of the cell cycle inhibitory protein p27 by phosphorylating Skp-2, the protein that regulates the level of p27,. Phosphorylation of Skp-2 prolongs the half-life of Skp-2, increases its levels, and enhances its ability to degrade p27. Pim also functions to stimulate the phosphorylation of the Cdc27 protein also inhibiting its function. Since active Cdc27 is needed for the destruction of Skp-2, this also increases Skp-2 and decreases the levels of p27. Low levels of p27 allow prostate cancer cells to rapidly transit the cell cycle. We find that our chemical inhibitor of Pim, SMI-4a, is able to reverse the activity of Pim-1 and increase the levels of p27. This data suggests that inhibition of Pim-1 by these agents would function to block prostate cancer growth by inhibiting transit through the cell cycle. Thus, our agent has potential activity to treat this cancer.

Table of Contents

INTRODUCTION (subject, purpose, and scope)

We have previously demonstrated using animal and tissue culture models that the overexpression of the Pim protein kinase even in transformed human prostate tumors will stimulate cell growth. In addition, others have demonstrated using Kaplan-Meier analysis that patients with a higher level of Pim are more prone to metastasis. We suggest that the c-Myc protooncogene works in concert with low levels of p27 to drive tumor growth. Further, we hypothesize that small molecule inhibitors of Pim protein kinase have the potential to reverse these effects. As a research team involving chemists and biologists, we have developed novel benzylidene thiazolidine-2,4 diones that inhibit Pim kinase activity and demonstrated that these compounds are capable of blocking Pim kinase activity both in tissue culture and in animals. The goal of these experiments is three fold. Our first goal is to understand the mechanism by which Pim protein kinases stimulate the cell cycle by regulating p27 levels. This work has led to a publication in The Journal of Biological Chemistry (see reportable outcomes) in which we describe the ability of Pim to phosphorylate both Skp-2 and Cdc27. The second goal of this work is to determine the mechanism by which Pim controls the levels of c-Myc and whether this correlates with the level of Pim protein kinases. The third goal is to evaluate whether maximal inhibition of tumor growth requires small molecule inhibition of all three Pim protein kinases.

BODY

Our research efforts have focused on specific portions of the Statement of Work, and in an attempt to bring together data that will satisfy the needs of a peer reviewed publication. This has led to a paper in the *Journal of Biological Chemistry* describing the effects of Pim on p27 levels and regulation by the ubiquitin degradation system. For the current work, we have focused on Task 3 parts 1 and 2. Although these tasks were not evaluated in the order of the prescribed Statement of Work, this analysis does form a coherent explanation for the activity of the Pim protein kinase. The results of these experiments are documented in a paper recently published in the *Proceedings of the National Academy of Sciences* that is attached. Rather than separating these tasks into individual goals for simplicity we have combined this description.

Task 3 to be completed in year 3: This task asked us to evaluate the interaction between the c-Myc protein and Pim kinase using our unique small molecule Pim inhibitor, SMI-4a. To evaluate this interaction, we have chosen to step back from the complicated prostate cancer models usually employed in Pim research, and attempt to initially simplify this analysis using MEFs from animals that are missing all of the 3 Pim kinase isoforms (triple knockout, TKO). Because there is no Pim kinase activity the biology of these cells mimics the effect of a small molecule Pim inhibitor with no off target effects. We find that the TKO cells do not grow well but expression of Pim 3 in these cells stimulated their growth similar to wild type cells (containing all 3 Pim isoforms) (Fig. 1). In contrast, Pim-2 stimulated intermediate growth and Pim-1 alone was not capable of stimulating the growth of these cells at all.

These results are of importance to the prostate cancer field because immunohistochemistry of human prostate cancers compared to normal paired samples from the same patient showed that Pim-3 was over expressed in prostate tumors (Fig. 2).

The TKO cells evidenced lower levels of ATP and higher amounts of AMP (Fig. 3a). The increased AMP is shown to phosphorylate the AMP-dependent protein kinase (AMPK) in these cells (Fig. 3b). Interestingly the over expression of Pim-3 is shown to reverse the levels of AMP:ATP, and to inhibit AMPK phosphorylation. Additionally, Pim-3 is shown to elevate the levels of c-Myc, both from MEFs derived from Pim-3 only mice and TKO MEFs that express Pim-3 after transduction (Fig. 4a, b). To examine how Pim-3 elevated the levels of c-Myc we first performed cycloheximide treatment and release of MEFs. Results demonstrated that TKO/Pim-3 cells synthesized more c-Myc at earlier time points (Fig. 5a). When a polysome profile analysis was carried out, c-Myc mRNA was found to associate with the polysomes in TKO/Pim-3 and WT MEFs, but in TKO MEFs the c-Myc mRNA was found to associate with free ribosomes (Fig. 5b), suggesting that 5′-cap-dependent translation was blocked in the absence of the Pims.

We also demonstrated that Pim-3 is capable of elevating the levels of the PGC-1α. (Fig. 6). Even though both c-Myc and Pim-3 increase the growth of TKO MEFs, only Pim-3 is able markedly increase the level of PGC-1α protein (Fig. 7a). Transduction of PGC-1α into TKO MEFs raised the levels of ATP and lowered the level of phosphorylated AMPK (Fig. 7b), suggesting that the ability of Pim-3 to control this enzyme is essential for its mechanism of action.

We therefore propose a model (Fig. 8) by which Pim-3 regulates PGC-1α, lowering the levels of AMP, stimulating mTORC1 activity and increasing the synthesis of c-Myc thus promoting the growth of these fibroblasts. We are in the process of validating this model in prostate cancer cells but initial results suggest that there is a significant degree of overlap. First, we find that the levels of Pim-3 are elevated in human prostate tumor samples by IHC. Second, PC-3 and LNCaP cells transfected with Pim-3 show increased ATP levels and higher growth rates than vector control cells.

KEY RESEARCH ACCOMPLISHMENTS

- **Knocking down Pim-1 or inhibiting its activity with the small molecule Pim inhibitor SMI-4a blocked mTORC1 activity.**
- **Inhibiting Pim-1 led to increases in AMP kinase activity, a known mTORC1 inhibitor.**
- **Mouse embryo fibroblasts (MEFs) which were knock-out for all three Pims (TKO) grew much more slowly than wild type and had elevated ratios of AMP:ATP**
- **TKO MEFs had elevated AMPK activity.**
- **These MEFs had decreased rates of protein synthesis and decreased levels of c-Myc protein.**
- **Elevating the levels of Pim-3 alone was sufficient to markedly increase growth, stimulate increases in c-Myc protein levels, and elevate the levels of PGC-1α.**
- **Transduction of PGC-1α was sufficient to elevate ATP and c-Myc protein.**

REPORTABLE OUTCOMES

Abstracts

Beharry Z, Lin Y, Mahajan S, Zemskova M, Xia Z, Smith C, Kraft AS. The Pim protein kinases modulate mTOR activity by regulating the protein and mRNA levels of mTOR pathway components and cellular AMP levels. AACR Special Conference in Cancer Research-Metabolism and Cancer. September 2009, La Jolla, CA.

Kraft AS, Beharry Z, Lin Y, Mahajan S, Zemskova M, Xia Z, Smith C. Treatment with the Pim protein kinase inhibitor SMI-4a enhances AMPK phosphorylation, decreases Raptor levels, and blocks mTORC1 activity. AACR Molecular Targets and Cancer Therapeutics Conference, 2009.

Papers

Cen B, Sandeep M, Zemskova M, Beharry Z, Lin YW, Cramer SD, Lilly M, and Kraft AS. Regulation of SKP2 Levels by the PIM-1 Protein Kinase. J Biol Chem. 285: 29128-29137, 2010.

Beharry Z, Mahajan S, Zemskova M, Lin Y-W, Tholanikunnel B, Xia Z, Smith CD, and Kraft AS. The Pim protein kinases regulate energy metabolism and cell growth. Proceedings of the National Academy of Sciences. 108:528-533, 2011.

CONCLUSIONS

The serine/threonine Pim kinases are overexpressed in prostate cancers and promote cell growth and survival. Here, we find that a novel Pim kinase inhibitor, SMI-4a, or Pim-1 siRNA blocked the rapamycin-sensitive mammalian target of rapamycin (mTORC1) activity by stimulating the phosphorylation and thus activating the mTORC1 negative regulator AMP-dependent protein kinase (AMPK). Mouse embryonic fibroblasts (MEFs) deficient for all three Pim kinases [triple knockout (TKO)] demonstrated activated AMPK driven by elevated ratios of AMP:ATP relative to wild type MEFs. Consistent with these findings, TKO MEFs were found to grow slowly in culture and have decreased rates of protein synthesis secondary to a diminished amount of 5′-cap–dependent translation. Pim-3 expression alone in TKO MEFs was sufficient to reverse AMPK activation, increase protein synthesis, and drive MEF growth similar to wild type. Pim-3 expression was found to markedly increase the protein levels of both c-Myc and the peroxisome proliferator-activated receptor gamma coactivator 1α (PGC-1α), enzymes capable of regulating glycolysis and mitochondrial biogenesis, which were diminished in TKO MEFs. Overexpression of PGC-1α in TKO MEFs elevated ATP levels and inhibited the activation of AMPK. These results demonstrate the Pim kinase-mediated control of energy metabolism and thus regulation of AMPK activity. We identify an important role for Pim-3 in modulating c-Myc and PGC-1α protein levels and cell growth. We find by IHC of human samples that Pim-3 is elevated in human prostate cancer, suggesting that these results will impact on human prostate cancer growth. Further experiments are being carried out to directly validate these findings in human prostate cancer.

APPENDIX A

The Pim protein kinases regulate energy metabolism and cell growth

Zanna Beharry[a], Sandeep Mahajan[b], Marina Zemskova[c], Ying-Wei Lin[d], Baby G. Tholanikunnel[b], Zuping Xia[a], Charles D. Smith[a,b], and Andrew S. Kraft[b,1]

[a]Department of Pharmaceutical and Biomedical Sciences, South Carolina College of Pharmacy, [b]Hollings Cancer Center, [c]Department of Cell and Molecular Pharmacology, and [d]Department of Pediatrics, Medical University of South Carolina, Charleston, SC 29425

Edited by Peter K. Vogt, The Scripps Research Institute, La Jolla, CA, and approved November 19, 2010 (received for review September 3, 2010)

The serine/threonine Pim kinases are overexpressed in solid cancers and hematologic malignancies and promote cell growth and survival. Here, we find that a novel Pim kinase inhibitor, SMI-4a, or Pim-1 siRNA blocked the rapamycin-sensitive mammalian target of rapamycin (mTORC1) activity by stimulating the phosphorylation and thus activating the mTORC1 negative regulator AMP-dependent protein kinase (AMPK). Mouse embryonic fibroblasts (MEFs) deficient for all three Pim kinases [triple knockout (TKO) MEFs] demonstrated activated AMPK driven by elevated ratios of AMP:ATP relative to wild-type MEFs. Consistent with these findings, TKO MEFs were found to grow slowly in culture and have decreased rates of protein synthesis secondary to a diminished amount of 5′-cap–dependent translation. Pim-3 expression alone in TKO MEFs was sufficient to reverse AMPK activation, increase protein synthesis, and drive MEF growth similar to wild type. Pim-3 expression was found to markedly increase the protein levels of both c-Myc and the peroxisome proliferator-activated receptor gamma coactivator 1α (PGC-1α), enzymes capable of regulating glycolysis and mitochondrial biogenesis, which were diminished in TKO MEFs. Overexpression of PGC-1α in TKO MEFs elevated ATP levels and inhibited the activation of AMPK. These results demonstrate the Pim kinase-mediated control of energy metabolism and thus regulation of AMPK activity. We identify an important role for Pim-3 in modulating c-Myc and PGC-1α protein levels and cell growth.

LKB1 | mitochondria | mTOR | 4EBP1

The Pim serine/threonine kinases include three isoforms, Pim-1, Pim-2, and Pim-3, that are implicated in the growth and progression of hematological malignancies, prostate cancer, and, in the case of Pim-3, in precancerous and cancerous lesions of the pancreas, liver, colon, and stomach (1–5). Pim-1 and Pim-2 have been shown to cooperate with c-Myc in inducing lymphoma (6), and prostate cancer (7), and in the absence of Pim-1 and Pim-2, Pim-3 is activated in c-Myc-induced lymphomas (8). The mechanisms suggested to explain this Pim–Myc synergism include Pim-mediated stabilization of c-Myc protein (9) and regulation of gene transcription via Pim-1 phosphorylation of histone H3 at active sites of c-Myc transcription (10). Other Pim kinase substrates that suggest these enzymes play a role in cell cycle progression and antiapoptosis include BAD, Bcl-2, Bcl-xL (11, 12), $p27^{Kip1}$ (13), and Cdc25A (14).

Recently, Pim kinases have been suggested to promote the activity of the rapamycin-sensitive mammalian target of rapamycin (mTORC1) (15–17). mTORC1 is a serine/threonine kinase that regulates cell growth and metabolism (18). The mTORC1 complex, composed of mTOR, raptor, GβL, and PRAS40, promotes protein synthesis by phosphorylating 4EBP1, thus stimulating its dissociation from the translational regulator eukaryotic initiation factor 4E (eIF4E) (17) allowing for cap-dependent translation. mTORC1 activity is regulated by a cascade of enzymes including LKB1, AMP-dependent protein kinase (AMPK), and TSC1 and 2 (19). AMPK senses the cellular energy status and is activated via LKB1-mediated phosphorylation when there is a decline in ATP levels and concomitant rise in AMP levels; i.e., high AMP:ATP ratio (20). Activated AMPK down-regulates the energetically demanding process of protein synthesis by inhibiting mTORC1 activity through phosphorylating TSC2 and raptor (20). The mechanisms by which Pim kinase stimulates mTORC1 appear complex and include 4EBP1, eIF4E (16, 21–23), and PRAS40 phosphorylation (15).

Because of the importance of the Pim kinase signal transduction pathway in the progression of various cancers, multiple groups have developed small-molecule inhibitors of this kinase family (24–28). We have identified unique benzylidene-thiazolidine-2-4-diones (23, 29) that inhibit Pim kinase activity in vitro at nanomolar concentrations, and in culture induce apoptosis of human leukemic cells (30) and synerigize with rapamycin to downregulate 4EBP1 phosphorylation and inhibit cell growth (29). Taking advantage of these inhibitors, siRNA, and genetically engineered Pim-deficient cells, we have discovered a unique role for Pim-3 in regulating mTORC1 activity through modulation of ATP levels by the induction of c-Myc and the transcriptional coactivator and master regulator of mitochondrial biogenesis peroxisome proliferator-activated receptor gamma coactivator 1α (PGC-1α).

Results

Pim Kinase Negatively Regulates AMPK. To examine the mechanisms by which Pim kinase can regulate the mTORC1 pathway, the human erythroleukemia cell line K562 was incubated with the thiazolidinedione Pim kinase inhibitor SMI-4a (23), and the phosphorylation of AMPK was studied. AMPK activation results in the phosphorylation of raptor and TSC2 and thus inhibits mTORC1 activity (20, 31). Pim kinase inhibition with SMI-4a induced the activation of AMPK as determined by phosphorylation of AMPKα at Thr172, and the AMPK targets acetyl-CoA carboxylase (ACC) at Ser79 and raptor at Ser792 and inhibition of mTORC1 activity as determined by decreased phosphorylation of the mTORC1 targets S6K and 4EBP1 (Fig. 1 *A* and *B*). Additionally, knockdown of Pim-1 levels with a targeted siRNA increased AMPK phosphorylation (Fig. 1*C*), suggesting that Pim-1 negatively regulates the phosphorylation of this enzyme. Because the LKB1 kinase is known to activate AMPK via phosphorylation at Thr172 (32) and loss of LKB1 activity is frequently associated with the transformed phenotype (32), we examined the ability of SMI-4a and SMI-16a, another Pim kinase inhibitor, (29) to regulate AMPK phosphorylation in a panel of LKB1-containing (H358, H661) and deficient (H23, H460, A549) lung cancer cell

Author contributions: Z.B. and A.S.K. designed research; Z.B., S.M., M.Z., Y.-W.L., and B.G.T. performed research; Z.B., S.M., M.Z., Y.-W.L., B.G.T., Z.X., and C.D.S. contributed new reagents/analytic tools; Z.B., S.M., M.Z., B.G.T., and A.S.K. analyzed data; and Z.B. and A.S.K. wrote the paper.

The authors declare no conflict of interest.

This article is a PNAS Direct Submission.

[1]To whom correspondence should be addressed. E-mail: kraft@musc.edu.

This article contains supporting information online at www.pnas.org/lookup/suppl/doi:10.1073/pnas.1013214108/-/DCSupplemental.

www.pnas.org/cgi/doi/10.1073/pnas.1013214108

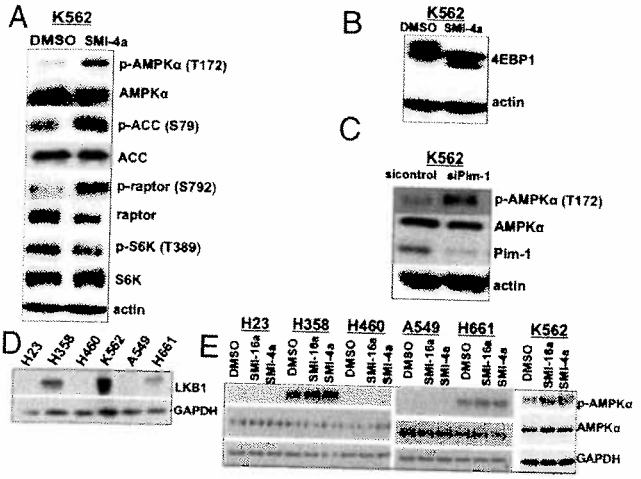

Fig. 1. Pim kinase inhibition activates AMPK. (*A* and *B*) K562 cells were treated with DMSO or SMI-4a (5 μM) for 1 h in the absence of serum, and lysates were probed for the indicated proteins by Western blotting. (*C*) K562 cells were transfected with scrambled siRNA (sicontrol) or Pim-1 siRNA (siPim-1), and 48 h later lysates were probed for the indicated proteins by Western blotting. (*D*) Western blot for LKB1 levels in lung cancer cell lines and the leukemia cell line K562. (*E*) Lung and leukemia cells were treated with DMSO, SMI-4a, or SMI-16a (5 μM) for 1 h in the absence of serum, and lysates were probed for the indicated proteins by Western blotting.

lines along with the LKB1-positive K562 cell line (Fig. 1*D*). These results demonstrate that the Pim kinase inhibitors SMI-4a and SMI-16a required LKB1 to stimulate AMPK activity (Fig. 1*E*).

To further confirm that Pim kinase regulates the activation of AMPK, we generated mouse embryonic fibroblasts (MEFs) deficient for Pim-1, -2, and -3 [triple knockout (TKO)] (33), and wild-type (WT) littermate control MEFs. Consistent with both the siRNA and small-molecule inhibition of Pim kinase activity, TKO MEFs had significantly higher AMPK phosphorylation compared to WT MEFs (Fig. 2*A*). To determine the contribution of each Pim isoform to AMPK activation, TKO MEFs were transduced with Pim-1, -2, or -3 lentiviruses. Although each Pim isoform reduced p-AMPK levels, Pim-3 showed the greatest effect (Fig. S1*A*) leading us to focus on elucidating the unique role of Pim-3. To confirm this result, we generated MEFs deficient in Pim-1 and Pim-2 (Pim-$1^{-/-}$, $-2^{-/-}$, $-3^{+/+}$) but expressing Pim-3, and demonstrated that these cells showed less activated AMPK than TKO MEFs (Fig. 2*A*). As AMPK activation is regulated by increased AMP, we measured the levels of AMP and ATP and found that AMPK phosphorylation correlates with the cellular AMP:ATP ratio in these knockout MEFs (Fig. 2*B*). Growth curves of these MEFs demonstrated a further correlation between proliferation, AMP:ATP ratio, and AMPK phosphorylation status (Fig. 2*C*) with the TKO MEFs showing the slowest growth rate. Similar results were obtained with immortalized WT or TKO MEFs transduced with empty vector or a lentivirus expressing Pim-3 (Fig. S1*B*).

Because activation of AMPK leads to inhibition of mTORC1 activity (31), we measured the level of protein synthesis in each of the MEFs. Labeling of MEFs with ^{35}S-methionine and measuring newly synthesized protein demonstrated, as predicted, that TKO MEFs when compared to WT have lower rates of protein synthesis (approximately 58% relative to WT). Expression of Pim-3 in the TKO cells increased protein synthesis from 58% (TKO) to 83% relative to WT (Fig. 2*D*). Consistent with this result, we found that in TKO MEFs the cap-dependent but not internal ribosome entry site (IRES)-dependent translational activity is reduced (Fig. 2*E*). Cap-dependent translation depends on the mTORC1-mediated release of 4EBP1 from eIF4E and the for-

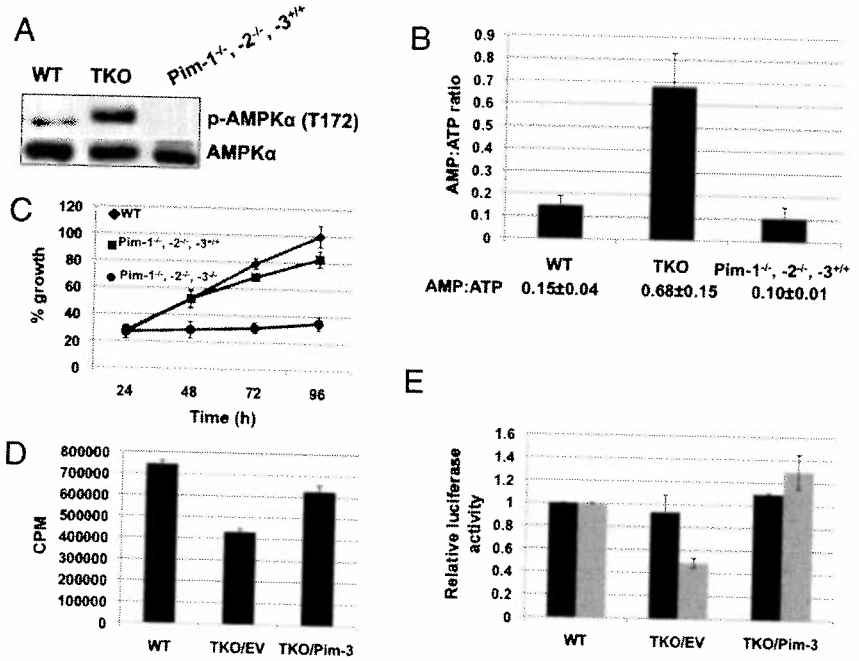

Fig. 2. Knockout of Pim kinase isoforms inhibits protein synthesis and cell growth. (*A*) Lysates were prepared from the different MEF cell lines and probed for the indicated proteins by Western blotting. (*B*) AMP:ATP ratios were determined by HPLC as described in *Materials and Methods*. Values are the average of three independent experiments, and the standard deviation from the mean is shown. (*C*) Growth curve of MEFs as determined by MTT assay. Percentage values are relative to the growth of WT MEFs at the 96 h time point (100%). The data points are the average of three independent measurements, and the standard deviation from the mean is shown. (*D*) ^{35}S-methionine incorporation into WT and TKO MEFs expressing empty vector (TKO/EV) or Pim-3 (TKO/Pim-3). Values (cpm/mg protein) are the average of three independent measurements, and the standard deviation for the mean is shown. (*E*) Cap-dependent (gray bars) and IRES-dependent (black bars) translation in MEFs as measured by Renilla and Firefly luciferase activities, respectively. As described in *Materials and Methods*, MEFs were infected with a virus expressing cap- and IRES-driven luciferase constructs. Values are the ratio of luciferase activity relative to WT and are the average of three independent measurements with the standard deviation from the mean shown.

mation of the eIF4F complex. Using m^7-GTP beads in a pull-down assay (34), we found that in TKO MEFs eIF4E is highly bound to 4EBP1, whereas eIF4G binding is lost and thus the ability of eIF4E to promote translation is inhibited (Fig. S1*C*). These results demonstrate that reduced Pim kinase activity correlates with increased AMP:ATP ratio, activation of AMPK, inhibition of mTORC1 activity, and reduced overall protein synthesis.

Pim-3 Regulates c-Myc Levels. In comparison to TKO MEFs, Pim-3–expressing cells demonstrated increased 5′-cap-dependent protein synthesis and growth similar to WT MEFs. Because the levels of the c-Myc protein are controlled by 5′-cap-dependent transcription, and c-Myc is important in the regulation of both cell growth and overall cellular metabolism, we examined the levels of c-Myc in MEFs from each genotype. Western blots demonstrate that the expression of Pim-3 either in primary MEFs (Fig. 3*A*) or after transduction into TKO MEFs (Fig. 3*B*) markedly increased c-Myc protein. Similar to p-AMPK (Fig. S1*A*), neither Pim-1 nor Pim-2 was able to induce the significant levels of c-Myc protein observed with Pim-3 overexpression in TKO MEFs (Fig. 3*B*). Furthermore, expression of Pim-1 or Pim-2 in Pim-3–only MEFs led to a decrease in c-Myc protein levels (Fig. S1*D*), suggesting the possibility that the Pim kinases could compete for substrates or interact directly. Because of the marked difference in c-Myc protein levels in MEFs containing Pim-3 only, we tested two additional MEF cell lines generated from different embryos of the same genotype and again observed increased c-Myc protein levels (Fig. S2*B*). To determine whether the increased c-Myc level in Pim-3–expressing cells is unique to MEFs in culture, we measured the c-Myc levels in spleen lysates of 4-mo-old WT, TKO, and Pim-$1^{-/-}$, -$2^{-/-}$, -$3^{+/+}$ mice and again found the highest level of c-Myc protein in the Pim-3–only genotype (Fig. S2*C*). Because deletion of one Pim might grossly elevate the level of another, in this case Pim-3, we measured the level of Pim-3 mRNA in the different MEF genotypes but did not find a significant difference (Fig. S2*A*). These results suggested that Pim-3 might modulate c-Myc translation.

To determine the effect of Pim-3 on c-Myc translation, we treated MEFs with cycloheximide until c-Myc protein was completely degraded, washed out the cycloheximide, and then monitored by Western blotting the rate of increase in c-Myc protein over time. To make this comparison possible, 2.5 times more protein from TKO MEFs was loaded on these SDS gels. TKO MEFs showed a delay in protein synthesis with only 53 and 43% as much c-Myc protein synthesis in the first 15 min when compared to WT and TKO/Pim-3 MEFS, respectively (Fig. 3*C*). This result is consistent with the reduced protein synthesis in the TKO MEFs (Fig. 2*D*). Because the overall translational efficiency in cells is reflected by changes in the polysome/monosome ratio, we determined the polysome profile using cytosolic extracts of WT, TKO, and TKO/Pim-3 cells. TKO cells showed a significant reduction in heavy polysomes and a corresponding increase in free ribosome subunits (Fig. 3*D Upper*). However, expression of Pim-3 in TKO cells resulted in a significant increase in heavy polysomes. c-Myc mRNA showed redistribution from heavy toward lighter polysomes and monosomes and free subunits in TKO cells relative to WT (Fig. 3*D Lower*). This shift was reversed by Pim-3 expression, suggesting that Pim-3 is capable of controlling the translation of c-Myc mRNA (Fig. 3*D Lower*). Because Pim-1 and -2 have been shown to increase the stability of c-Myc (9), we examined changes in c-Myc protein stability in TKO and TKO/Pim-3 MEFs after cycloheximide treatment but found no significant difference in c-Myc half-life in the Pim-3–containing cells (Fig. S2*D*). Finally, we found that the expression of c-Myc in TKO MEFs led to a decrease in AMPK activation (Fig. S2*E*) consistent with the ability of c-Myc to stimulate cell growth.

Pim-3 and c-Myc Regulate PGC-1α Levels. The differences in the growth rate between the TKO and Pim-3 only MEFs could possibly be explained by the Pim-3–mediated increased c-Myc because the latter is known to control multiple factors that regulate cell growth and metabolism (35, 36). Therefore, we compared the growth rate of TKO MEFs stably expressing empty vector, Pim-3, or c-Myc to WT MEFs. The TKO/c-Myc MEFs were able to

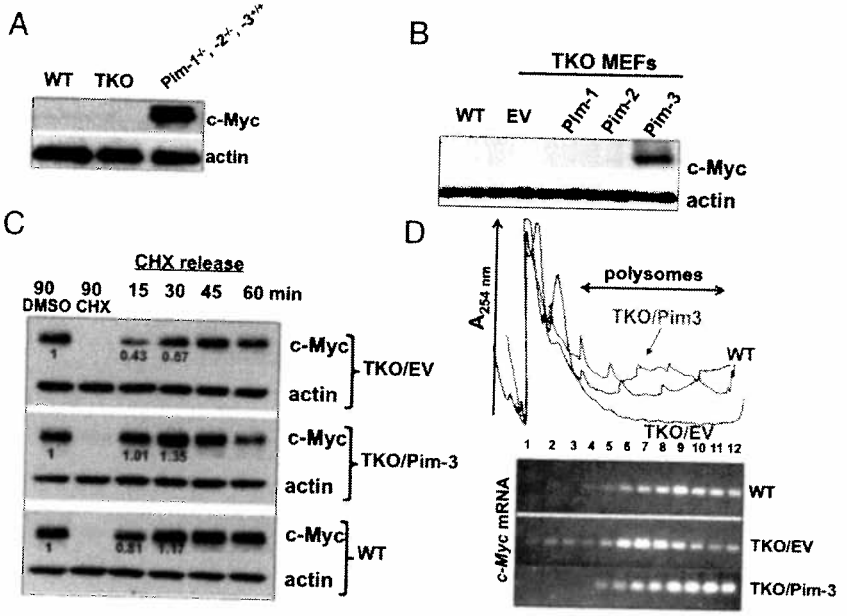

Fig. 3. Pim-3 elevates c-Myc levels. (*A*) c-Myc protein levels in each MEF genotype as determined by Western blotting. (*B*) TKO MEFs were infected with empty vector (EV), Pim-1, -2, or -3 lentiviruses, and 48 h later lysates were probed for c-Myc levels and compared to WT MEFs. (*C*) TKO MEFs expressing EV or Pim-3 were treated for 90 min with cycloheximide (CHX, 10 μM), the media replaced, and lysates probed for c-Myc levels by Western blotting. Densitometry analysis was performed, and the values at the 15 min time point relative to DMSO are shown. To obtain a relatively equal amount of c-Myc protein at the 90 min time point with DMSO, ~2.5-fold more TKO/EV protein lysate was loaded relative to TKO/Pim-3. (*D*) Ribosome fractions of WT and TKO MEFs expressing EV or Pim-3 were prepared by sucrose gradient (see *Materials and Methods*), and the level of c-Myc mRNA associated with each fraction was determined by PCR.

grow in the absence of Pim kinases but did not reach the same density in 96 h (Fig. 4*A*). The shRNA-mediated knockdown of c-Myc in TKO/Pim-3 MEFs did not completely inhibit cell proliferation (Fig. 4*B*). Together, these results suggest that Pim-3 and c-Myc do not have completely overlapping biologic activities. To understand how Pim-3 decreases the AMP:ATP ratio and inhibits AMPK phosphorylation, we measured the levels of PGC-1α. PGC-1α activates a wide variety of transcription factors that result in increased mitochondrial biogenesis and oxidative phosphorylation (37). Increased expression of PGC-1α can lead to elevations in ATP levels (38), whereas PGC-1α knockout leads to reduced ATP levels in murine hearts (39). PGC-1α expression and PGC-1α–dependent gene expression are induced by chemical activation of AMPK, and AMPK directly phosphorylates PGC-1α, leading to increased transcriptional activity (40–42). We found that the levels of PGC-1α mRNA and protein were greatly reduced in TKO MEFs, highest in Pim-3–only MEFs, and intermediate in WT cells (Fig. 4*C* and *D*). To examine the contributions of Pim-3 and c-Myc in regulating PGC-1α levels, we infected TKO MEFs with lentiviruses expressing c-Myc or Pim-3 and found that Pim-3 induced marked increases in PGC-1α mRNA (12-fold) and protein; the effect of c-Myc alone was a 4-fold increase in mRNA, and the increase in protein was quantitated at only 10% that of Pim-3 (Fig. 4*D*, *E*).

The above results suggest that the increased AMP:ATP ratio in TKO MEFs may be attributed to low ATP levels due to decreased PGC-1α protein, thus leading to AMPK activation. To examine whether overexpression of PGC-1α in TKO MEFs was sufficient to reduce p-AMPK by increasing the level of cellular ATP, we transduced TKO MEFs with a lentivirus expressing PGC-1α. Western blots and biochemical analysis demonstrate that PGC-1α expression in TKO MEFs decreased the level of p-AMPK (Fig. 5*A*) and increased the levels of ATP (Fig. 5*B*), leading to decreased 4EBP1 binding to eIF4E while increasing eIF4G association with the eIF4E protein (Fig. S3). In contrast, PGC-1α expression in TKO MEFs showed little effect on c-Myc levels (Fig. 5*A*). Thus, Pim-3, by controlling the levels of both c-Myc and PGC-1α, is able to impact on AMPK phosphorylation, mTORC1 activity, 5′-cap-dependent translation, and ultimately cell growth (Fig. 5*C*).

Discussion

The combined approach of genetic knockout, RNAi, and small-molecule inhibition implicate the Pim kinases in regulating the AMP:ATP ratio and energy metabolism. These effects lead to the modulation of the mTORC1 pathway by AMPK and the control of cell growth. In leukemic cells, the pan-Pim kinase inhibitor SMI-4a stimulated the phosphorylation and activation of AMPK, whereas in TKO MEFs the ratio of AMP:ATP was markedly increased and AMPK was activated. Because AMPK is a negative regulator of mTORC1, we found in leukemic cells treated with SMI-4a and in TKO MEFs that mTORC1 activity is inhibited and cap-dependent translation is significantly decreased. In MEFs, the expression of Pim-3 alone could reverse these processes, lowering the AMP:ATP ratio, decreasing the activation of AMPK, and increasing cap-dependent translation, all resulting in cellular growth rates comparable to WT MEFs. The differences between the TKO and Pim-3–only MEFs could be explained in part by the Pim-3–mediated increased c-Myc because the latter controls multiple transcription factors that regulate cell growth and metabolism (35, 36). Infection of TKO MEFS with a lentivirus expressing c-Myc increased the growth of these cells but did not duplicate the growth curve of Pim-3–expressing MEFs.

In muscle and fat tissue, the ability of activated AMPK to maintain an energy balance is achieved in part by stimulating PGC-1α (41). The ability of PGC-1α to coactivate multiple transcription factors makes this protein a master regulator of mitochondrial biogenesis (43). Considering this link between

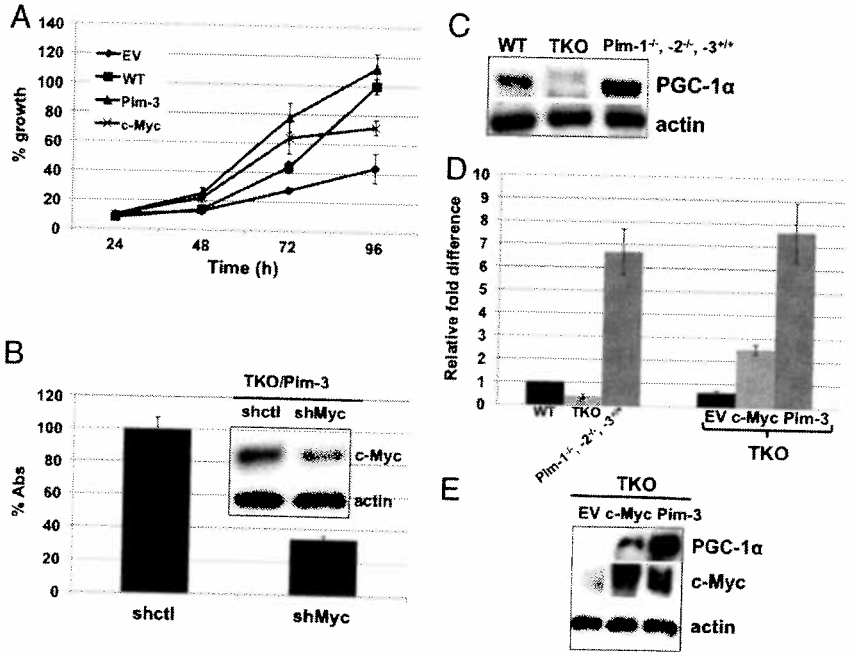

Fig. 4. Pim-3 and c-Myc affect PGC-1α levels. (*A*) Growth curve of TKO MEFs expressing empty vector (EV), c-Myc, or Pim-3 as determined by an MTT assay. Percentage values are relative to the value of WT MEFs at the 96 h time point (100%). The data points are the average of three independent measurements, and the standard deviation from the mean is shown. (*B*) TKO/Pim-3 MEFs were infected with nontargeting shRNA (shctl) or c-Myc targeting shRNA (shMyc) lentiviruses. Equal numbers of shctl and shMyc cells were plated 48 h postinfection, and after an additional 72 h viability was determined by an MTT assay and represented as a percent absorbance (%Abs) with shctl set at 100%. The data points are the average of three independent measurements, and the standard deviation from the mean is shown. (*Inset*) Lysates were prepared at 120 h postinfection and probed for the indicated proteins by Western blotting. (*C*) PGC-1α protein levels in MEFs as determined by Western blotting. (*D*) PGC-1α mRNA levels in primary MEFs (WT, TKO, Pim-1$^{-/-}$, -2$^{-/-}$, -3$^{-/-}$) or TKO MEFs infected with EV, c-Myc, or Pim-3 lentiviruses as determined by QT-PCR 48 h after infection. Values are the average of three independent measurements, and the standard deviation from the mean is shown. (*E*) PGC-1α protein levels as determined by Western blotting in TKO MEFs 48 h postinfection with EV, c-Myc, or Pim-3.

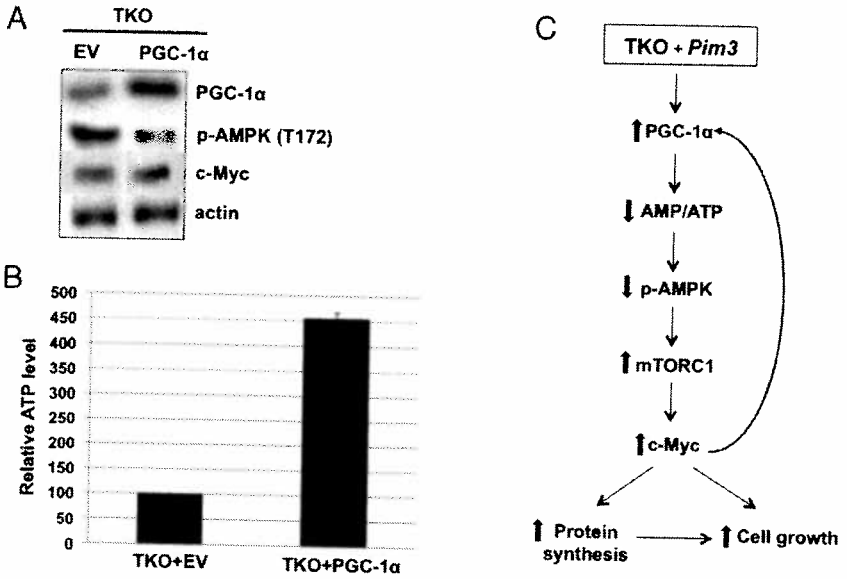

Fig. 5. Expression of PGC-1α restores the AMP:ATP ratio in TKO MEFs. (*A*) PGC-1α overexpression in TKO MEFs reduces AMPK activation. Lysates were prepared from TKO MEFs 48 h after transduction with empty vector (EV) or PGC-1α lentiviruses, and protein levels compared by Western blotting. (*B*) ATP levels determined in lysates from Fig. 5*A* as described in *Materials and Methods*. Values are the average of three independent measurements, and the standard deviation from the mean is shown. (*C*) Schematic summary of biologic changes observed in TKO MEFs expressing Pim-3.

AMPK and PGC-1α in the sensing and regulation of the cell's energy status, the levels of PGC-1α were investigated and found to be significantly lower in TKO MEFs. In comparison, Pim-3–containing MEFs showed increased levels of PGC-1α relative to WT. Therefore, in the case of the TKO MEFs, chronic AMPK activation coupled with drastically reduced levels of PGC-1α protein resulted in an elevated AMP:ATP ratio. Accordingly, infection of TKO MEFs with a lentivirus expressing PGC-1α was shown to increase ATP levels and decrease AMPK activation. The increased PGC-1α levels in Pim-3–only MEFs cannot be attributed solely to increased c-Myc because TKO/c-Myc MEFs showed lower levels of PGC-1α mRNA and protein relative to TKO/Pim-3 MEFs. This suggests the possibility that Pim-3 and c-Myc could cooperate in regulating PGC-1α levels in MEFs. This cooperation may extend beyond transcription/translation because PGC-1α levels and activity are regulated by multiple posttranslational mechanisms (37).

Pim-3 is the least-studied kinase of the Pim family; however, it has been linked to the development and progression of colon and pancreatic cancers (2–4, 44). Despite the high sequence identity and overlapping substrate specificity of the Pim kinases, Pim-3 expression alone is shown to overcome at least some of the defects found in the loss of both Pim-1 and Pim-2, including growth rate. Additionally, the knockout of Pim-1 and -2 and the expression of Pim-3 only led to a marked increase in c-Myc protein relative to WT MEFs. The observation that the transduction of Pim-1 or -2 into MEFs containing Pim-3 suppressed c-Myc levels suggested the possibility that individual Pim isoforms may regulate each other either directly or through substrate competition. This poses the question of whether Pim isoforms either individually or acting in concert regulate different biological processes and under what cellular circumstances. The question of the activity of Pim isoforms is of importance to the design of small-molecule inhibitors targeting these kinases and their use in the treatment of diseases, including cancer. Both Pim-1 and -2 are known to enhance c-Myc–induced transformation (6, 12) and phosphorylate and stabilize c-Myc protein, leading to increased transcriptional activity (9). In the MEFs used in this study, Pim-3 expression alone enhanced cap-dependent translation, increased c-Myc levels without changing the protein's stability, and increased the cell growth rate. Because elevated levels of both Pim-3 and c-Myc are found in gastrointestinal cancers, our results suggest the possibility that Pim-3 might enhance the growth of these tumor cells in part by regulating c-Myc levels, thus highlighting the potential utility of Pim-3 targeted inhibitors.

Materials and Methods

Cell Culture. MEFs were derived from 14.5-d-old embryos and were genotyped as described (45). For stable cell lines, TKO MEFs were transduced with lentiviruses encoding empty vector, PIM-1, Pim-2, Pim-3, or c-Myc and selected with puromycin (4 μg/mL).

Construction of Lentiviral Vectors. The open reading frames of PIM-1 (human, 33 kDa isoform), PIM-2 (mouse), Pim-3 (mouse), c-Myc (mouse), and PGC-1α (human, a gift from Young-In Chi, Department of Molecular and Cellular Biochemistry, University of Kentucky, Lexington, KY) were amplified by PCR from full-length cDNA clones and subcloned into the *AgeI-MluI* sites of pLex-MCS lentiviral vector (Open Biosystems). Methods for preparation of lentiviral stocks are detailed in *SI Materials and Methods*.

Quantitative RT-PCR (QT-PCR). Total RNA was isolated from MEFs using the RNeasy kit (Qiagen) according to the manufacturer's protocol. The first-strand cDNA was synthesized using Superscript first-strand synthesis kit and Oligo (dT) primer (Invitrogen).

Biochemical Analysis. K562 cells were transfected with scrambled siRNA or siPim-1 (ON-TARGETplus SMARTpool, Thermo Scientific) using Lipofectamine™2000 (Invitrogen) according to the manufacturer's protocol, and 48 h posttransfection lysates were prepared. Cell growth was measured using the 3-(4,5-dimethylthiazol-2-yl)-2,5-diphenyl tetrazolium bromide (MTT) assay. ATP, ADP, and AMP were measured by HPLC as described previously (46), and ATP was also measured using the ATP Bioluminescence Assay Kit HS II (Roche) with 10^5 cells. eIF4E was captured on m^7-GTP sepharose (GE Lifesciences) from WT and TKO MEFs lysate and bound 4EBP1 and eIF4G determined by Western blotting.

^{35}S-Methionine Incorporation. Cells were serum starved for 1 h in methionine-free medium (Invitrogen), followed by labeling with 100 mCi of ^{35}S-methionine/mL. Lysates and labeled proteins were precipitated with trichloroacetic acid on glass microfiber filters (Whatman) using vacuum filtration, and ^{35}S-incorporation was counted.

Cap- vs. IRES-Dependent Translation. A bicistronic retroviral vector, pMSCV/rLuc-pol IRES-fLuc (a gift from Peter B. Bitterman, Department of Medicine, University of Minnesota, Minneapolis, MN), was used to produce viral particles for infecting WT, TKO and TKO/Pim-3 MEFs. Cells were collected

48 hr postinfection and Renilla/Firefly luciferase activities were quantified using the dual-luciferase reporter assay system (Promega) and a luminometer according to the manufacturer's instructions.

Polysome Profile Analysis. Sucrose density gradient centrifugation was employed to separate the ribosome fractions as described previously (47). c-Myc mRNA level in each fraction was measured by PCR.

1. Shah N, et al. (2008) Potential roles for the PIM1 kinase in human cancer—A molecular and therapeutic appraisal. *Eur J Cancer* 44:2144–2151.
2. Fujii C, et al. (2005) Aberrant expression of serine/threonine kinase Pim-3 in hepatocellular carcinoma development and its role in the proliferation of human hepatoma cell lines. *Int J Cancer* 114:209–218.
3. Li YY, et al. (2006) Pim-3, a proto-oncogene with serine/threonine kinase activity, is aberrantly expressed in human pancreatic cancer and phosphorylates bad to block bad-mediated apoptosis in human pancreatic cancer cell lines. *Cancer Res* 66:6741–6747.
4. Popivanova BK, et al. (2007) Proto-oncogene, Pim-3 with serine/threonine kinase activity, is aberrantly expressed in human colon cancer cells and can prevent Bad-mediated apoptosis. *Cancer Sci* 98:321–328.
5. White E (2003) The pims and outs of survival signaling: Role for the Pim-2 protein kinase in the suppression of apoptosis by cytokines. *Genes Dev* 17:1813–1816.
6. Allen JD, Verhoeven E, Domen J, van der Valk M, Berns A (1997) Pim-2 transgene induces lymphoid tumors, exhibiting potent synergy with c-myc. *Oncogene* 15:1133–1141.
7. Wang J, et al. (2010) Pim1 kinase synergizes with c-MYC to induce advanced prostate carcinoma. *Oncogene* 29:2477–2487.
8. Mikkers H, et al. (2002) High-throughput retroviral tagging to identify components of specific signaling pathways in cancer. *Nat Genet* 32:153–159.
9. Zhang Y, Wang Z, Li X, Magnuson NS (2008) Pim kinase-dependent inhibition of c-Myc degradation. *Oncogene* 27:4809–4819.
10. Zippo A, De Robertis A, Serafini R, Oliviero S (2007) PIM1-dependent phosphorylation of histone H3 at serine 10 is required for MYC-dependent transcriptional activation and oncogenic transformation. *Nat Cell Biol* 9:932–944.
11. Macdonald A, et al. (2006) Pim kinases phosphorylate multiple sites on Bad and promote 14-3-3 binding and dissociation from Bcl-XL. *BMC Cell Biol* 7:1.
12. Shirogane T, et al. (1999) Synergistic roles for Pim-1 and c-Myc in STAT3-mediated cell cycle progression and antiapoptosis. *Immunity* 11:709–719.
13. Morishita D, Katayama R, Sekimizu K, Tsuruo T, Fujita N (2008) Pim kinases promote cell cycle progression by phosphorylating and down-regulating p27Kip1 at the transcriptional and posttranscriptional levels. *Cancer Res* 68:5076–5085.
14. Bachmann M, et al. (2006) The oncogenic serine/threonine kinase Pim-1 directly phosphorylates and activates the G2/M specific phosphatase Cdc25C. *Int J Biochem Cell Biol* 38:430–443.
15. Zhang F, et al. (2009) PIM1 protein kinase regulates PRAS40 phosphorylation and mTOR activity in FDCP1 cells. *Cancer Biol Ther* 8:846–853.
16. Hammerman PS, Fox CJ, Birnbaum MJ, Thompson CB (2005) Pim and Akt oncogenes are independent regulators of hematopoietic cell growth and survival. *Blood* 105:4477–4483.
17. Laplante M, Sabatini DM (2009) mTOR signaling at a glance. *J Cell Sci* 122:3589–3594.
18. Gibbons JJ, Abraham RT, Yu K (2009) Mammalian target of rapamycin: Discovery of rapamycin reveals a signaling pathway important for normal and cancer cell growth. *Semin Oncol* 36:S3–S17.
19. Bai X, Jiang Y (2010) Key factors in mTOR regulation. *Cell Mol Life Sci* 67:239–253.
20. Shaw RJ (2009) LKB1 and AMP-activated protein kinase control of mTOR signalling and growth. *Acta Physiol* 196:65–80.
21. Chen WW, Chan DC, Donald C, Lilly MB, Kraft AS (2005) Pim family kinases enhance tumor growth of prostate cancer cells. *Mol Cancer Res* 3:443–451.
22. Lilly M, Kraft A (1997) Enforced expression of the Mr 33,000 Pim-1 kinase enhances factor-independent survival and inhibits apoptosis in murine myeloid cells. *Cancer Res* 57:5348–5355.
23. Xia Z, et al. (2009) Synthesis and evaluation of novel inhibitors of Pim-1 and Pim-2 protein kinases. *J Med Chem* 52:74–86.

ACKNOWLEDGMENTS. We thank Yefim Manevich and Robin Muise-Helmericks (Medical University of South Carolina) for technical assistance. We are grateful to Anton Berns (Netherlands Cancer Institute) and Paul B. Rothman (University of Iowa Medical Center) for the generous gift of Pim TKO mice. We also thank Vortex Biotechnology for providing the Pim kinase inhibitors used in this study. This work was supported in part by Department of Defense Grant W81XWH-08-PCRP-IDA, and the shared resources are supported by the Hollings Cancer Center.

24. Pogacic V, et al. (2007) Structural analysis identifies imidazo[1,2-b]pyridazines as PIM kinase inhibitors with in vitro antileukemic activity. *Cancer Res* 67:6916–6924.
25. Akue-Gedu R, et al. (2009) Synthesis, kinase inhibitory potencies, and in vitro antiproliferative evaluation of new Pim kinase inhibitors. *J Med Chem* 52:6369–6381.
26. Chen LS, Redkar S, Bearss D, Wierda WG, Gandhi V (2009) Pim kinase inhibitor, SGI-1776, induces apoptosis in CLL lymphocytes. *Blood* 114:4150–4157.
27. Grey R, et al. (2009) Structure-based design of 3-aryl-6-amino-triazolo[4,3-b]pyridazine inhibitors of Pim-1 kinase. *Bioorg Med Chem Lett* 19:3019–3022.
28. Tong Y, et al. (2008) Isoxazolo[3,4-b]quinoline-3,4(1H,9H)-diones as unique, potent and selective inhibitors for Pim-1 and Pim-2 kinases: Chemistry, biological activities, and molecular modeling. *Bioorg Med Chem Lett* 18:5206–5208.
29. Beharry Z, et al. (2009) Novel benzylidene-thiazolidine-2,4-diones inhibit Pim protein kinase activity and induce cell cycle arrest in leukemia and prostate cancer cells. *Mol Cancer Ther* 8:1473–1483.
30. Lin Y, et al. (2009) A small molecule inhibitor of Pim protein kinases blocks the growth of precursor T-cell lymphoblastic leukemia/lymphoma. *Blood* 115:824–833.
31. Gwinn DM, et al. (2008) AMPK phosphorylation of raptor mediates a metabolic checkpoint. *Mol Cell* 30:214–226.
32. Hezel AF, Bardeesy N (2008) LKB1; linking cell structure and tumor suppression. *Oncogene* 27:6908–6919.
33. Mikkers H, et al. (2004) Mice deficient for all PIM kinases display reduced body size and impaired responses to hematopoietic growth factors. *Mol Cell Biol* 24:6104–6115.
34. Connolly E, Braunstein S, Formenti S, Schneider RJ (2006) Hypoxia inhibits protein synthesis through a 4E-BP1 and elongation factor 2 kinase pathway controlled by mTOR and uncoupled in breast cancer cells. *Mol Cell Biol* 26:3955–3965.
35. Liu YC, et al. (2008) Global regulation of nucleotide biosynthetic genes by c-Myc. *PLoS One* 3–e2722.
36. Li F, et al. (2005) Myc stimulates nuclearly encoded mitochondrial genes and mitochondrial biogenesis. *Mol Cell Biol* 25:6225–6234.
37. Canto C, Auwerx J (2009) PGC-1alpha, SIRT1 and AMPK, an energy sensing network that controls energy expenditure. *Curr Opin Lipidol* 20:98–105.
38. Liang H, Bai Y, Li Y, Richardson A, Ward WF (2007) PGC-1alpha-induced mitochondrial alterations in 3T3 fibroblast cells. *Ann NY Acad Sci* 1100:264–279.
39. Arany Z, et al. (2005) Transcriptional coactivator PGC-1 alpha controls the energy state and contractile function of cardiac muscle. *Cell Metab* 1:259–271.
40. Suwa M, Nakano H, Kumagai S (2003) Effects of chronic AICAR treatment on fiber composition, enzyme activity, UCP3, and PGC-1 in rat muscles. *J Appl Physiol* 95:960–968.
41. Jäger S, Handschin C, St.-Pierre J, Spiegelman BM (2007) AMP-activated protein kinase (AMPK) action in skeletal muscle via direct phosphorylation of PGC-1α. *Proc Natl Acad Sci USA* 104:12017–12022.
42. Irrcher I, Ljubicic V, Kirwan AF, Hood DA (2008) AMP-activated protein kinase-regulated activation of the PGC-1alpha promoter in skeletal muscle cells. *PLoS One* 3:e3614.
43. Finley LW, Haigis MC (2009) The coordination of nuclear and mitochondrial communication during aging and calorie restriction. *Ageing Res Rev* 8:173–188.
44. Li YY, Wu Y, Tsuneyama K, Baba T, Mukaida N (2009) Essential contribution of Ets-1 to constitutive Pim-3 expression in human pancreatic cancer cells. *Cancer Sci* 100:396–404.
45. Xu J (2005) Preparation, culture, and immortalization of mouse embryonic fibroblasts. *Curr Protoc Mol Biol* Chap 28: Unit 28.1.
46. Hahn-Windgassen A, et al. (2005) Akt activates the mammalian target of rapamycin by regulating cellular ATP level and AMPK activity. *J Biol Chem* 280:32081–32089.
47. Ishimaru D, et al. (2009) Regulation of Bcl-2 expression by HuR in HL60 leukemia cells and A431 carcinoma cells. *Mol Cancer Res* 7:1354–1366.

Supporting Information

Beharry et al. 10.1073/pnas.1013214108

SI Materials and Methods

Reagents and Cell Culture. The following antibodies were used in this study and were obtained from Cell Signaling (CS) or Santa Cruz Biotechnology (SC): p-AMPKα (T172) (CS2535), AMPKα (CS2532), p-ACC (S79) (CS3661), ACC (CS3676), p-raptor (S792) (CS2083), raptor (CS2280), p-S6K (CS9206), S6K (CS9202), Pim-1 (SC28777), p-4EBP1 (T37/46) (CS2855), 4EBP1 (CS9452), LKB1 (SC28788), eIF4E (CS9742), mTOR (CS2983), Pim-2 (SC13514), Pim-3 (SC98959), c-Myc (CS9402), PGC-1α (SC13067), eIF4G (CS2498). Additional antibodies were purchased from other sources: actin (Sigma A3854), and GAPDH (Sigma G9295). Mouse embryonic fibroblasts (MEFs), K562, and lung cancer cell lines were cultured in DMEM containing 10% fetal bovine serum.

Construction of Lentiviral Vectors and Preparation of Lentiviral Stocks. Lentiviral shRNA constructs (nontargeting shctl and Pim-3 targeting, shPim-3) were purchased from Open Biosystems. Lentiviral particles were produced by transfecting 293Tcells in a 10-cm dish with 9 mg of lentiviral plasmid, 28.5 mg of translentiviral packaging mix (Open Biosystems), and 187.5 mg of transfection reagent, Express-in (Open Biosystems) according to the manufacturer's recommendations. Forty-eight hours after transfection, viral supernatants were collected, filtered, concentrated 25-fold by centrifugation at 50,000 × *g* at 4 °C for 3 h, and aliquots were stored at −80 °C. The titers of the concentrated viral particles were measured with a p24 ELISA kit (Cell Biolabs, Inc.) and found to be between 10^6–10^8 transduction units (TU)/mL. For transduction, 1×10^6 cells were infected with 10^6 TU of viral stock using the Viraductin, lentiviral transduction kit (Cell Biolabs, Inc.) according to the manufacturer's recommendations. Forty-eight hours later, cells were harvested, lysed, and protein expression analyzed by SDS-PAGE followed by Western blotting.

Biochemical Analysis. Relative quantification of gene expression was achieved by quantitative real-time PCR (iQ5 Multicolor Real-Time PCR detection system, BioRad Laboratories) using iQ5 optical system software. The expression levels were normalized to GAPDH. The primers used for real-time PCR are listed below.

Pim-3. Forward TGTGGTCTCTGGGTGTACTGCG
Reverse GACACCACTCAATAAGCTGCTGG

PGC-1α. Forward GAATCAAGCCACTACAGACACCG
Reverse CATCCCTCTTGAGCCTTTCGTG

GAPDH. Forward CCCACTAACATCAAATGGGG
Reverse ATCCACAGTCTTCTGGGTGG

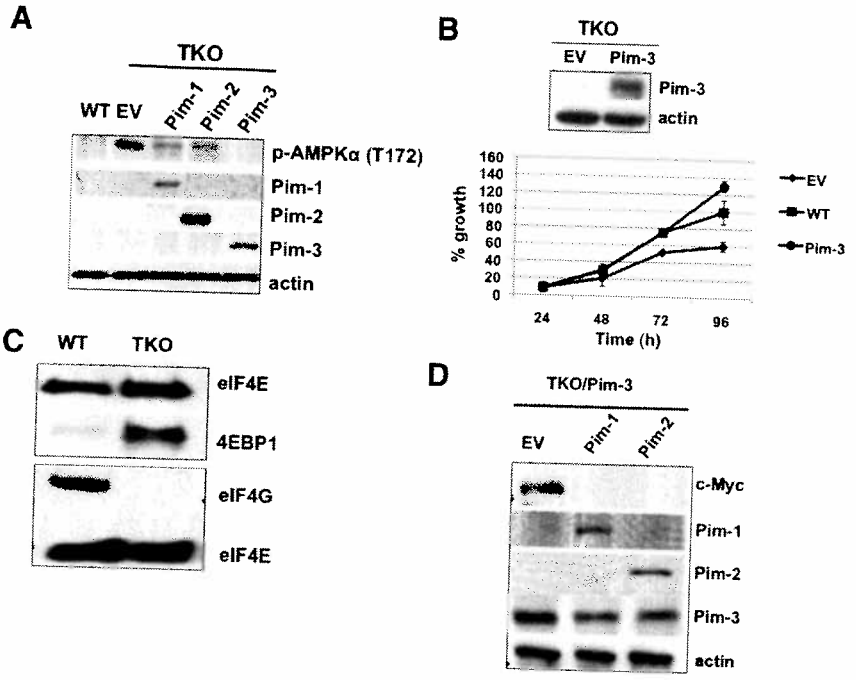

Fig. S1. (*A*) Lysates were prepared 48 h after transduction with empty vector (EV), Pim-1, -2, or -3 lentiviruses and probed for the indicated proteins. The levels in wild-type MEFs (WT) are shown for comparison. (*B*) Expression of Pim-3 in stable cell lines used for growth curve analysis (*Upper*). Growth curve of TKO MEFs infected with EV or Pim-3 as determined by a 3-(4,5-dimethylthiazol-2-yl)-2,5-diphenyl tetrazolium bromide (MTT) assay. Percentage values are relative to the value of WT MEFs at the 96 h time point (100%). The data points are the average of three independent measurements, and the standard deviation from the mean is shown. (*C*) 4EBP1 binding to eIF4E is increased, while eIF4G binding to eIF4E is decreased in TKO MEFs. eIF4E was captured on m^7-GTP resin from WT and TKO MEFs lysate, and the levels of bound 4EBP1 and eIF4G were determined by Western blotting. (*D*) TKO/Pim-3 MEFs were infected with EV, Pim-1, or Pim-2 lentiviruses, and 48 h later lysates were probed for c-Myc and Pim kinase levels.

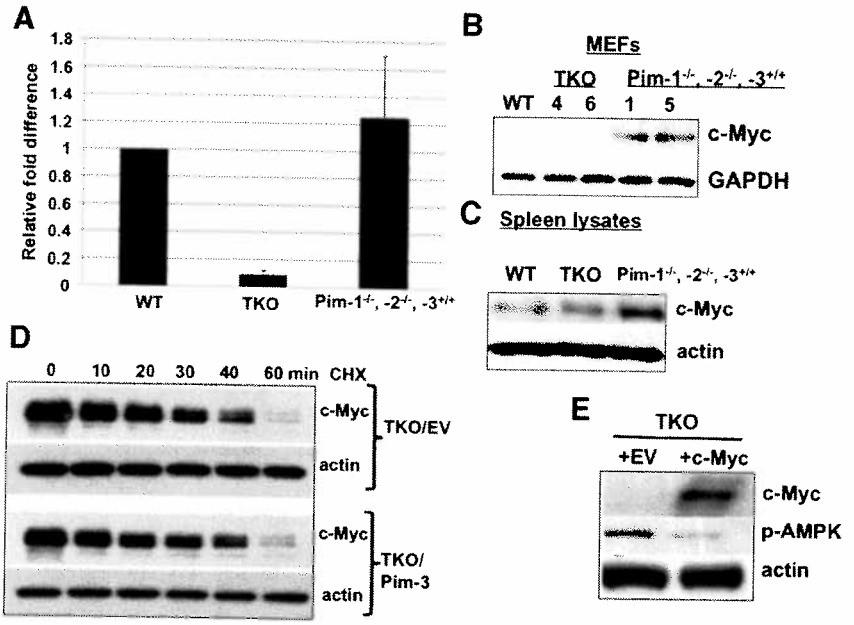

Fig. S2. (*A*) Pim-3 mRNA levels in each of the MEFs determined by quantitative RT-PCR. Values are the average of three independent measurements, and the standard deviation from the mean is shown. (*B*) c-Myc protein levels in WT, TKO, and Pim-3–only MEFs as determined by Western blotting with GAPDH as a loading control. MEFs were generated as described in *Materials and Methods* and were derived from separate embryos. These MEFs were not used for the experiments shown in the main text and only serve to validate that the increased c-Myc protein levels in the Pim-1$^{-/-}$, -2$^{-/-}$, -3$^{-/-}$ cells are not unique to a single MEF cell line. (*C*) Spleen lysates from age-matched WT and TKO mice were probed for c-Myc protein. (*D*) c-Myc protein stability in TKO MEFs expressing empty vector (EV) or Pim-3. Cells were treated with cycloheximide (CHX, 10 μM) and lysates prepared at the indicated time points and probed for c-Myc protein levels. To obtain a relatively equal amount of c-Myc protein at the 0 min time point, ~2.5-fold more TKO/EV protein lysate was loaded relative to TKO/Pim-3. (*E*) Lysates were prepared after 48 h transduction with EV or c-Myc lentiviruses and probed for the indicated proteins.

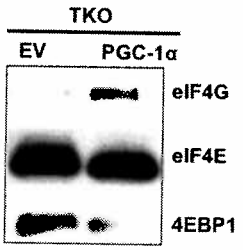

Fig. S3. TKO MEFs were infected with empty vector (EV) or PGC-1α lentiviruses, and 48 h later eIF4E was captured on m^7-GTP resin and binding to eIF4G and 4EBP1 was determined.

SUPPORTING DATA

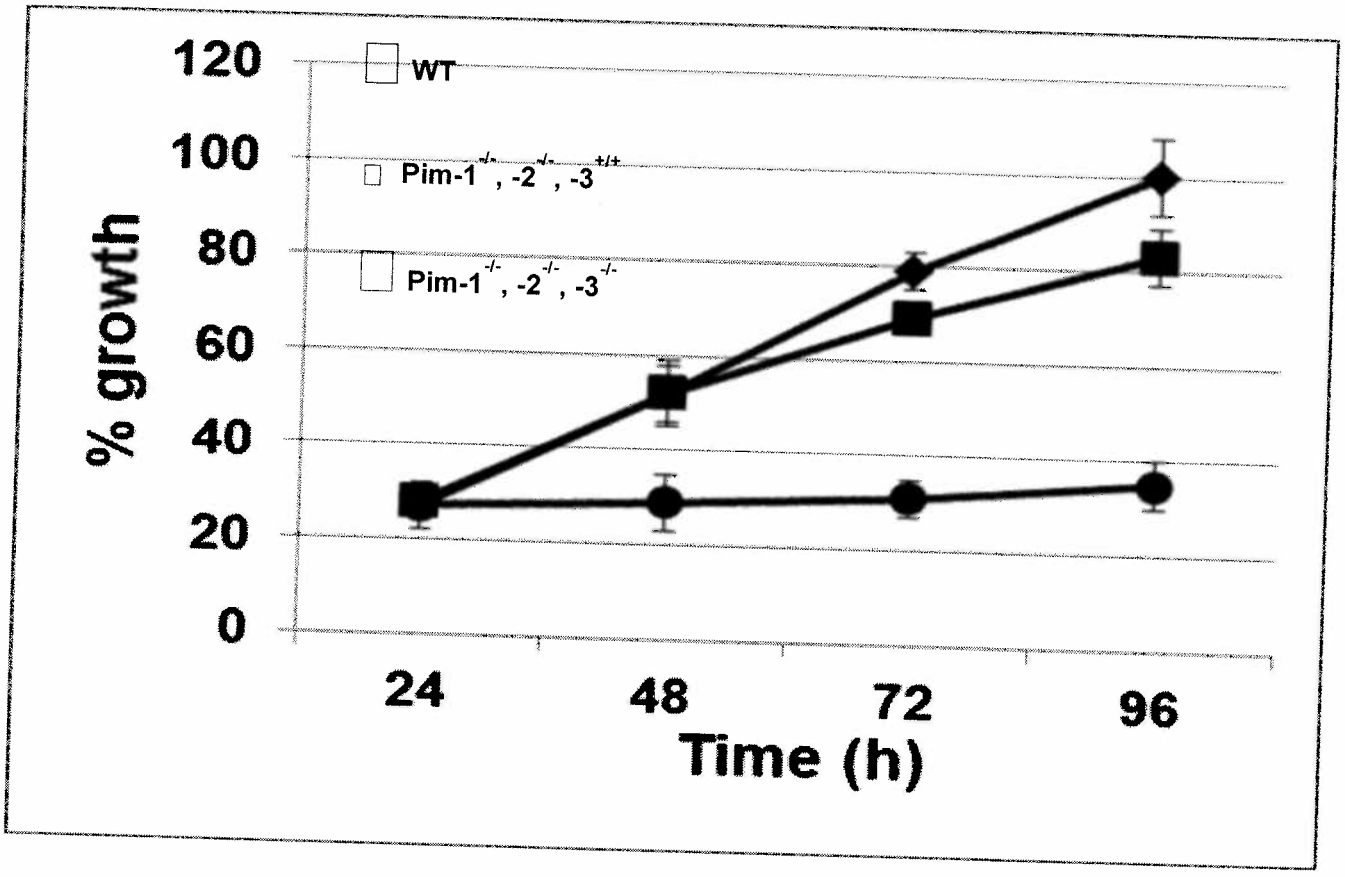

Fig. 1: Growth curve of MEFS as determined by the MTT assay. Percentage values are relative to the growth of WT MEFs at the 96h time point (100%). The data points are the average of three independent measurements, and the standard deviation from the mean is shown.

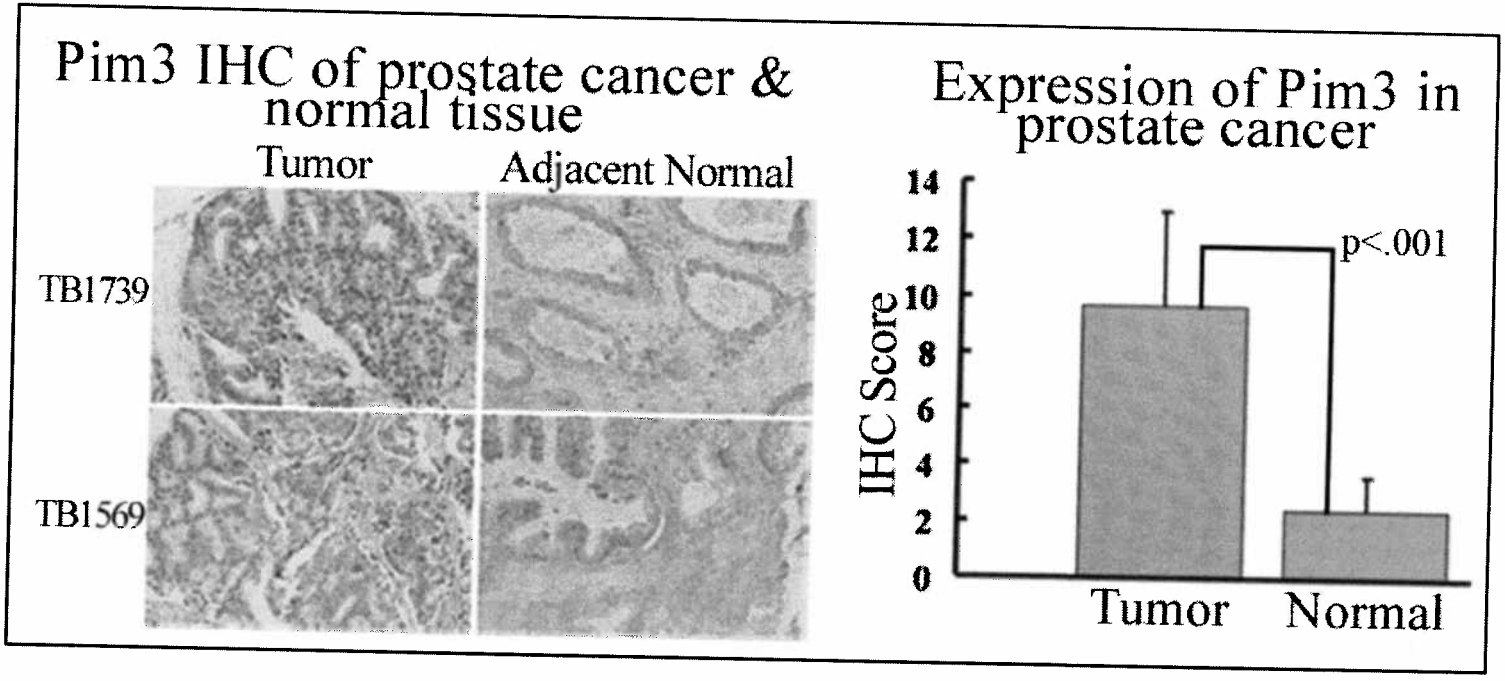

Fig. 2: Expression of Pim-3 in human prostate cancer. (A) Representative IHC staining of Pim-3 using a prostate tissue microarray with 26 adenocarcinomas and paired adjacent normal tissues. (B) Semi-quantitative analysis of IHC. Percentage staining was scored on a scale of 0-4, where 0=no positive cells, 1=1-25% positive cells, 2=26-50% positive cells, 3=51-75% positive cells, and 4=76-100% positive cells. The intensity of staining was scored on a scale of 0-3, where 0=negative, 1=mild, 2=moderate, and 3=intensive staining. A final score was calculated by multiplying the percentage and intensity scores. The average of all tissues examined is shown with the standard deviation from the mean.

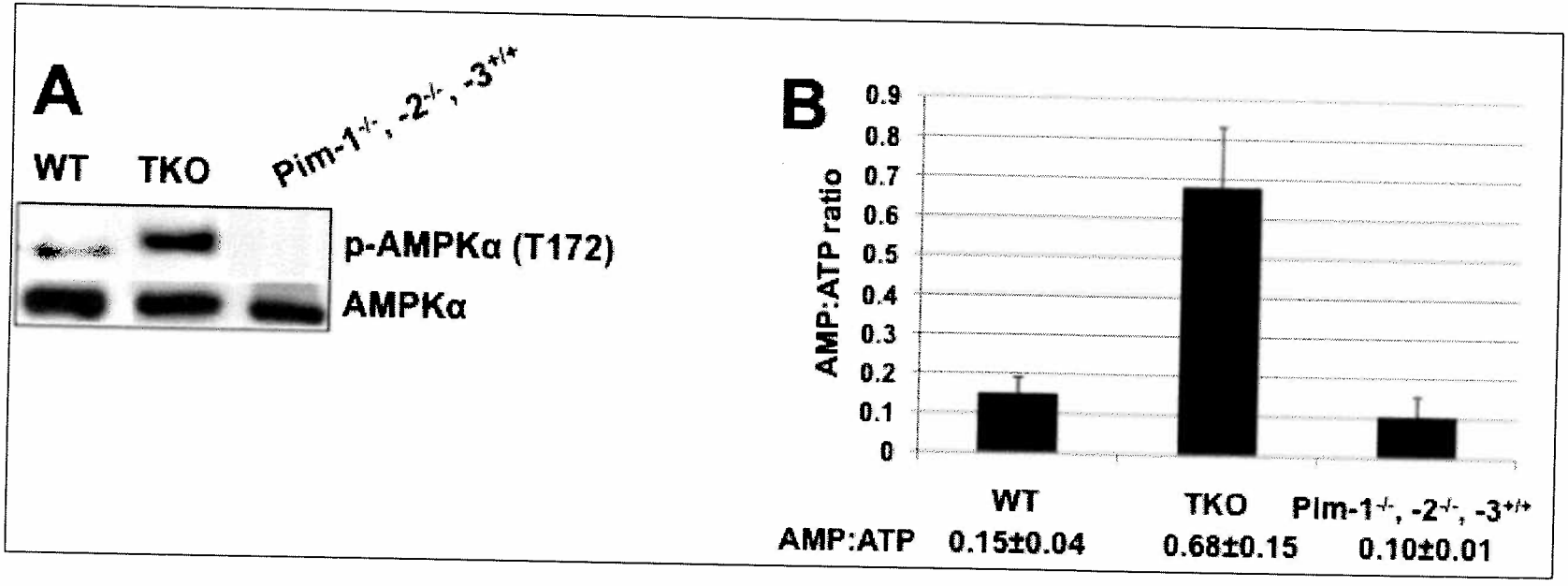

Fig. 3. (A) AMP:ATP ratios were determined by HPLC. Values are the average of three independent experiments, and the standard deviation from the mean is shown. **(B)** Lysates were prepared from the different MEF cell lines and probed for the indicated proteins by Western blotting.

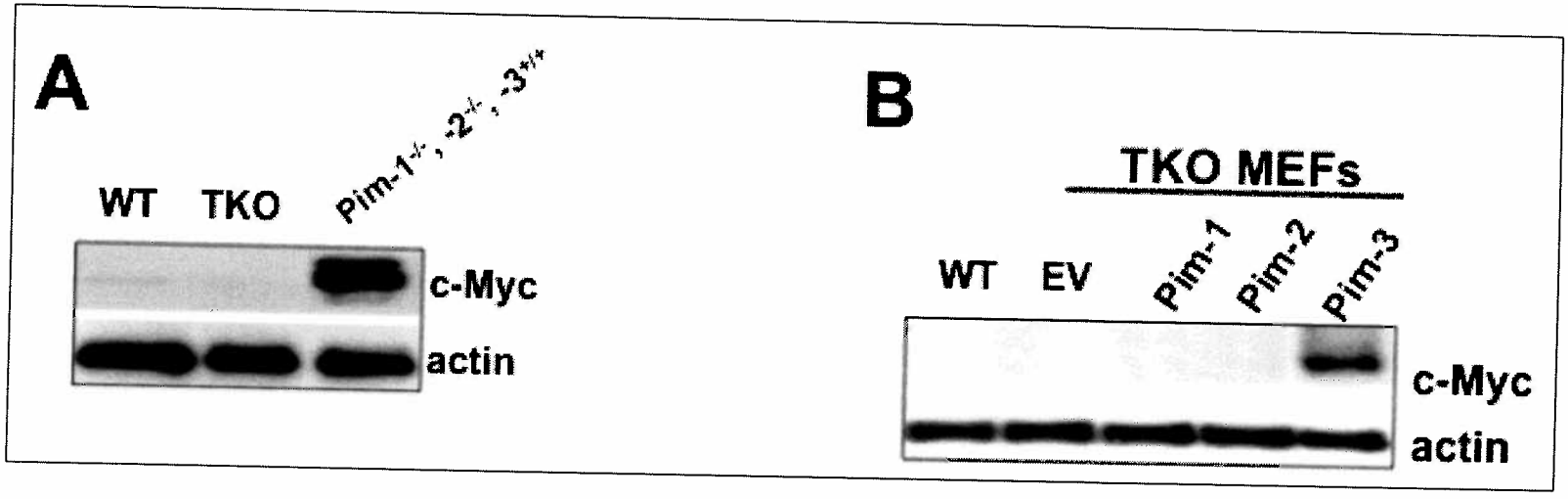

Fig. 4: (A) c-Myc protein levels in each MEF genotype as determined by Western blotting. **(B)** TKO MEFs were infected with empty vector (EV) Pim 1,2, and 3 lentiviruses, and 48 h later lysates were probed for c-Myc levels and compared to WT MEFs.

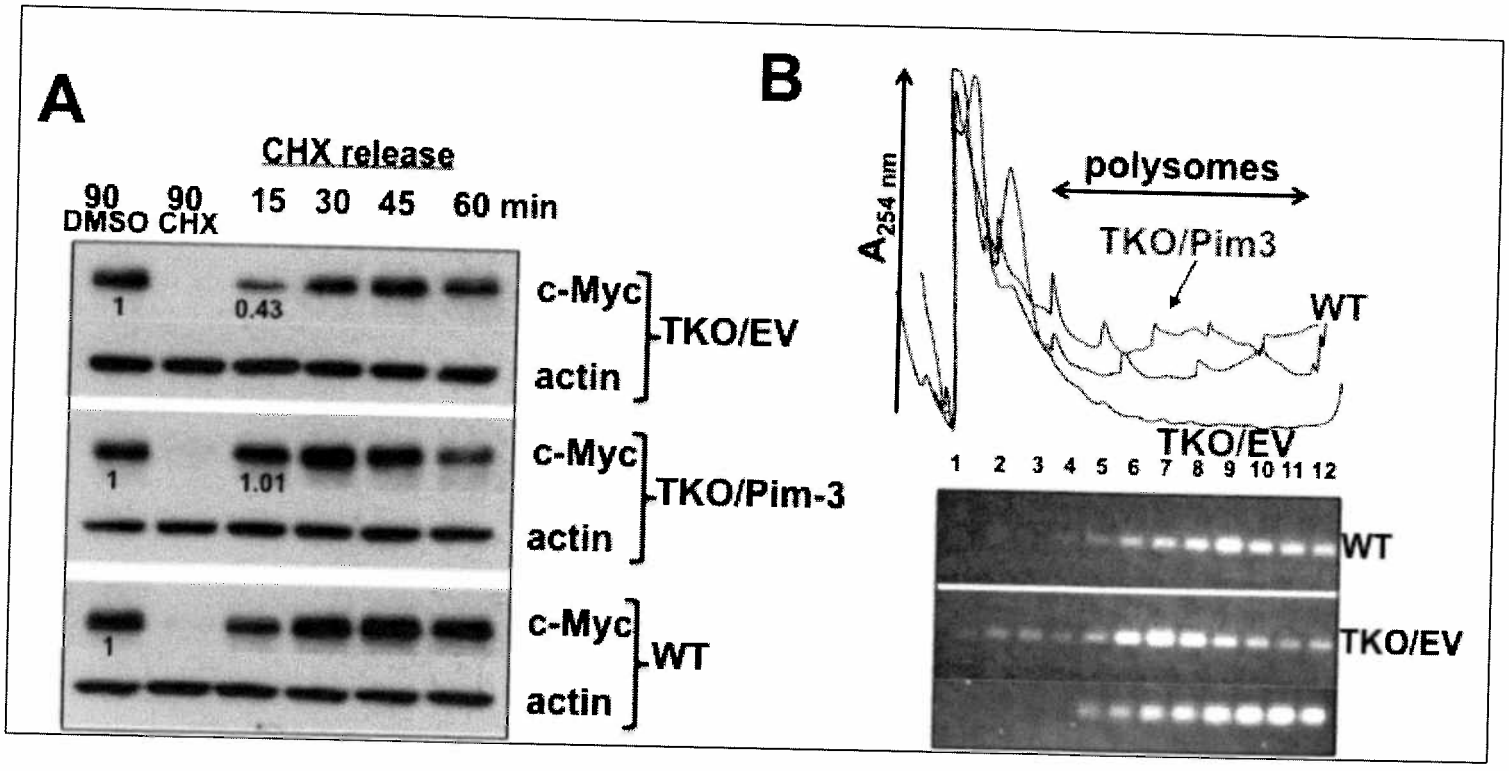

Fig. 5: TKO **(A)** MEFs expressing empty vector, Pim-3 or WT were treated for 90 min with cycloheximide , media replaces, and lysates probed for c-Myc levels by Western blotting. Densitometry was done and the values at the 15 and 30 min time points are shown. **(B)** Ribosome fractions of WT and TKO MEFs expressing EV or Pim-3 were prepared by sucrose gradient, and the level of c-Myc mRNA associated with each fraction was determined by PCR.

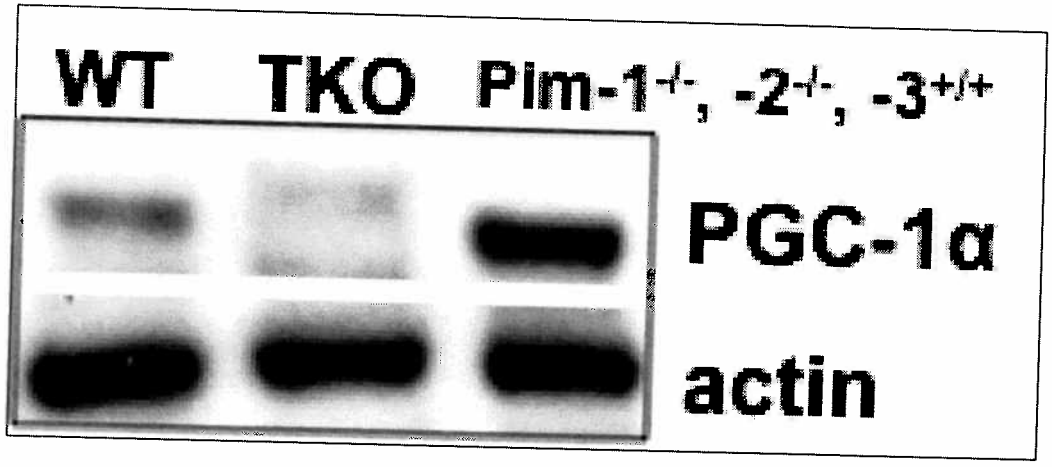

Fig. 6: PGC-1α protein levels in MEFs as determined by Western blotting.

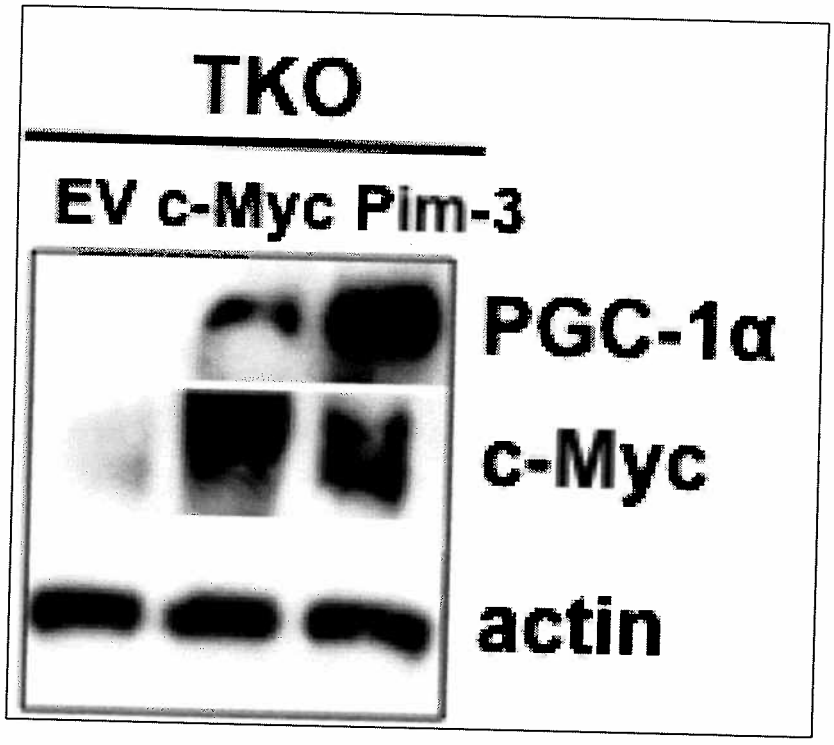

Fig. 7. PGC-1α protein levels as determined by Western blotting in TKO MEFs 48 h postinfection with EV, c-Myc, or Pim-3.

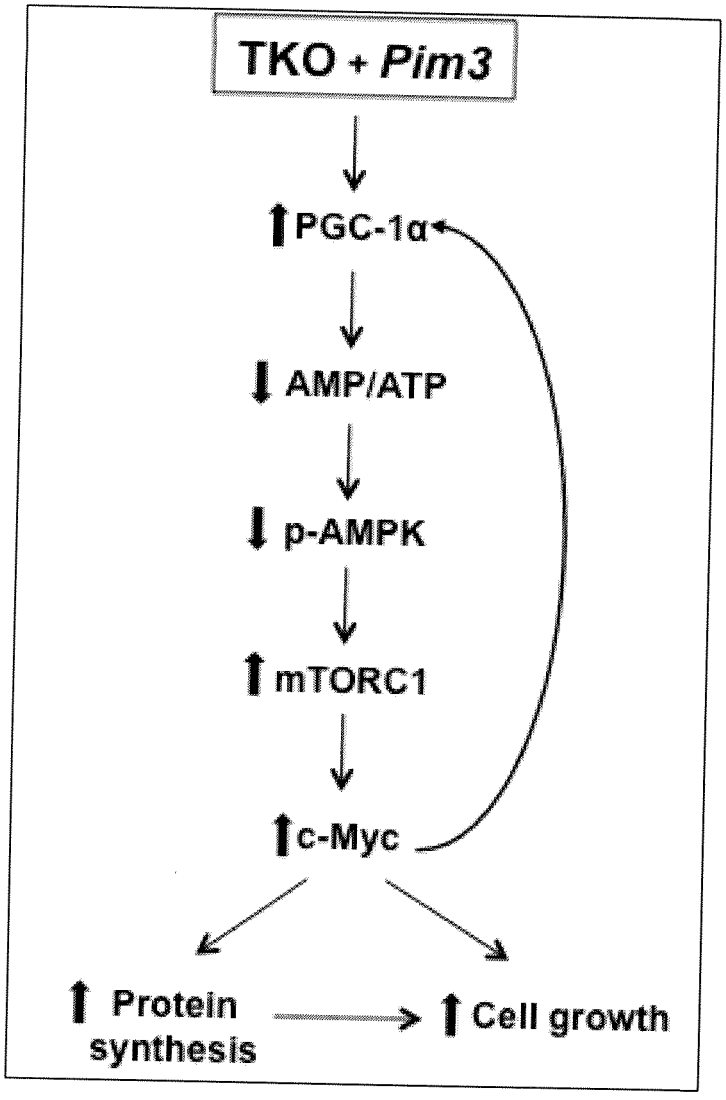

Fig. 8. Schematic summary of biologic changes observed in TKO MEFs expressing Pim-3.